

Charge Fluctuations in Superconducting Mesoscopic Contacts

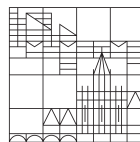
Doctor's Thesis

by

Oliver Irtenkauf

at the

Universität
Konstanz



Faculty of Science
Department of Physics

1. Reviewer: Prof. Dr. Elke Scheer
2. Reviewer: Prof. Dr. Juan Carlos Cuevas

Konstanz, 2025

Zusammenfassung

Hier könnte Ihre Zusammenfassung stehen.

Abstract

Please insert abstract here.

Kleines Statement ¹

Hineinfließen
in die Formen,
die sich stellen.
Sich aber nicht
formen lassen
und auf keinen Fall
erhärten.

Das wäre
Leben
für mich.

¹Kristiane Allert-Wybranietz (*1955)

Contents

1	Theory	1
1.1	Introduction to Superconductivity	1
1.1.1	London	1
1.1.2	Ginzburg Landau	1
1.1.3	BCS Theory	1
1.1.4	Josephson Effect	1
1.2	Josephson Junction	1
1.3	Andreev Reflection	1
1.4	Multiple Andreev Reflection	1
2	Methods	2
2.1	Sample Design	2
2.1.1	Sample Design	3
2.1.2	shadow evaporation	3
2.2	Setup	3
2.2.1	cryostat and thermometer	3
2.2.2	MCBJ	3
2.2.3	DC Cabling	3
2.2.3.1	copper powder filter	3
2.2.3.2	steel capillary cable	3
2.2.3.3	comercial silver epoxy filter	3
2.2.4	AC cabling	3
2.2.4.1	Antenna	3
2.2.4.2	stripline	3
2.3	Data Aqucition	3
2.3.1	Measurement Concept	3
2.3.2	Measurement Software	3
2.4	Data Threadment	3
2.4.1	data filtering	3
3	Atomic Contacts	4

4 Tunnelbarrier	5
5 Appendix	i
6 Theory	iii
6.1 Landau-Lifshitz-Gilbert Model	iii
6.2 Kittel Formula	v
6.3 Co-planar Waveguide	vi
References	vii

1 Theory

1.1 Introduction to Superconductivity

1.1.1 London

1.1.2 Ginzburg Landau

1.1.3 BCS Theory

1.1.4 Josephson Effect

1.2 Josephson Junction

1.3 Andreev Reflection

1.4 Multiple Andreev Reflection

2 Methods

278.8371pt3.85902in 3.85902in

2.1 Sample Design

general idea

2.1.1 Sample Design

2.1.2 shadow evaporation

2.2 Setup

2.2.1 cryostat and thermometer

2.2.2 MCBJ

2.2.3 DC Cabling

2.2.3.1 copper powder filter

2.2.3.2 steel capillary cable

2.2.3.3 comercial silver epoxy filter

2.2.4 AC cabling

2.2.4.1 Antenna

2.2.4.2 stripline

2.3 Data Aqucition

2.3.1 Measurement Concept

2.3.2 Measurement Software

2.4 Data Threadment

2.4.1 data filtering

3 Atomic Contacts

cmd + C, shake, cmd + V

4 Tunnelbarrier

Asymmetrien. Viel Spaß ein Video in einzelbildern zu printen

5 Appendix

Figure 1

Figure 2

Program 1

Program 1 Listing Caption is above.

```
1 """version from 15.12.23
2 author: Oliver Irtenkauf
3
4 features: Coporate Design Colors of University Konstanz
5 and inverse colors for more contrast
6
7 """
8
9 import numpy as np
10 import matplotlib.pyplot as plt
11
12 x = np.linspace(0, 1, 1001)
13 y = 3 * x
14 plt.plot(x, y)
15 plt.plot(x, x**2)
```

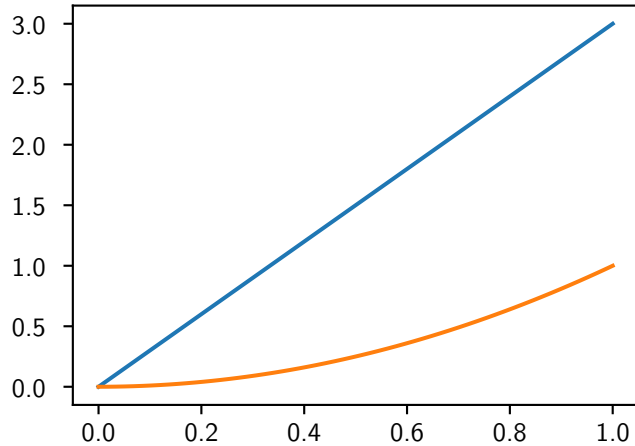


Figure 1 Complex susceptibility

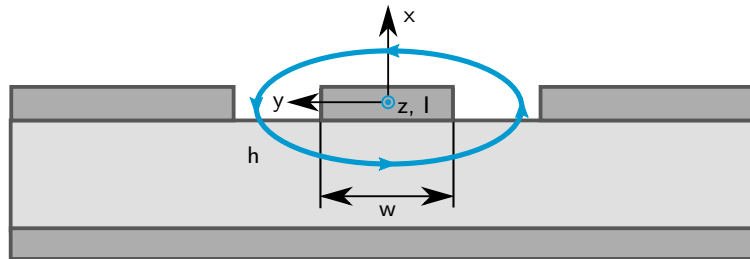


Figure 2 blablabla.

6 Theory

In this Chapter in order to understand the ferromagnetic resonance (FMR) technique I want to recall some basic concepts of magneto dynamics. Furthermore, I also want to give a short excursion into the coherence lengths of singlet and triplet Cooper pairs, since they are needed to define my samples dimensions reasonably. Finally, I want to present you the current state of the art, in the field of FMR measurements on thin ferromagnetic films.

6.1 Landau-Lifshitz-Gilbert Model

The dynamic magnetic properties of a ferromagnet can be described by damped precessional motion of the exchange-coupled magnetic moments. If the externally applied magnetic fields and excitation energies are significantly smaller than the exchange coupling energy, we can describe the whole ferromagnet as a macroscopic magnetic spin by the Landau-Lifshitz-Gilbert (LLG) model.

The LLG differential equation for the magnetization \vec{M} is given by

$$\frac{d\vec{M}}{dt} = \underbrace{-|\gamma|(\vec{M} \times \mu_0 \vec{H}_{\text{eff}})}_{(1)} + \underbrace{\frac{\alpha}{|\vec{M}|} \left(\vec{M} \times \frac{d\vec{M}}{dt} \right)}_{(2)}, \quad (6.1)$$

where γ is the gyro-magnetic ratio, α is the Gilbert damping parameter and μ_0 is the vacuum permeability. The effective magnetic field is given by $\vec{H}_{\text{eff}} = \vec{H} + \vec{H}_{\text{ani}}$, with \vec{H} being the externally applied magnetic field and \vec{H}_{ani} the anisotropy field.

For better understanding of the LLG model, we first neglect the Gilbert damping term (2) in equation 6.1. With this neglection the LLG equation simply describes the precession of the magnetization \vec{M} around the effective field \vec{H}_{eff} . Here the gyro-magnetic ratio is given by $\gamma_e = \frac{g_e \mu_B}{\hbar} = \frac{g_e q_e}{2m_e}$, where \hbar is the reduced Planck constant, μ_B the Bohr magneton, g_e , q_e

and m_e describe the g -factor, charge and mass of the free electron respectively. Since the magnetism in ferromagnets, especially in Co, is caused by the electron spins, we can assume a g -factor $g \approx 2$ and thus a gyromagnetic ratio of $\frac{\gamma}{2\pi} = 28.025 \text{ GHz T}^{-1}$. The precession frequency ω_{res} is given by

$$\omega_{\text{res}} = \gamma \mu_0 |\vec{H}_{\text{eff}}|, \quad (6.2)$$

resulting in typical resonance frequencies $\omega_{\text{res}}/2\pi$ in the GHz range, for a few Tesla of applied external magnetic field.

Now we consider the phenomenological Gilbert term (2) from equation 6.1. After the displacement of \vec{M} , it precesses in a spiral trajectory back to its equilibrium position. This relaxation is due to the scattering of phonons and magnons and can be characterised by the relaxation rate κ . This rate is related to the frequency linewidth by $\Delta\omega = \frac{1}{2\kappa}$, where the linewidth $\Delta\omega$ is usually defined as full width at half maximum (FWHM) and κ as the inverse of the half width at half maximum (HWHM). Now the linewidth $\Delta\omega$ is connected to the Gilbert parameter α by

$$\Delta\omega = 2\alpha\omega_{\text{res}} + \Delta\omega_0. \quad (6.3)$$

The inhomogeneous broadening $\Delta\omega_0$ is caused by magnetic inhomogeneities or surface effects.

In order to solve the LLG differential equation 6.1 we will neglect for now the field anisotropy $\vec{H}_{\text{ani}} = 0$. To this end we split the applied magnetic field \vec{H} and magnetization \vec{M} into static (\vec{H}_0, \vec{M}_0) and dynamic (\vec{h}, \vec{m}) components.

$$\vec{H} = \vec{H}_0 + \vec{h}(t) \quad (6.4)$$

$$\vec{M} = \vec{M}_0 + \vec{m}(t) \quad (6.5)$$

Next we assume a static magnetic field in z -direction and a dynamic field in x - and y -direction $\vec{H} = (h_x(t), h_y(t), H_0)$. If the dynamic magnetic field is much smaller than the static magnetic field, we can also write for the magnetization $\vec{M} = (m_x(t), m_y(t), M_0)$. Here is M_0 the absolute static magnetization. The solution is given by $\vec{m} = \chi \vec{h}$. The two-dimensional Polder tensor χ is given by

$$\chi = \begin{pmatrix} \chi_{11} & i\chi_{12} \\ -i\chi_{12} & \chi_{22} \end{pmatrix}. \quad (6.6)$$

Since we neglect magnetic field anisotropy, the diagonal elements are the same $\chi = \chi_{11} = \chi_{22}$. Further, we neglect every higher damping

therm $\mathcal{O}(\alpha^2)$, in order to get the linear response of a ferromagnet in an external field. Finally, the Polder susceptibility is then given by

$$\chi(\omega, H_0) = \frac{\omega_M (\gamma\mu_0 H_0 - i\Delta\omega)}{(\omega_{\text{res}}(H_0))^2 - \omega^2 - i\omega\Delta\omega}. \quad (6.7)$$

Here is the magnetization frequency $\omega_M = \gamma\mu_0 M_0$ and the resonance frequency ω_{res} . In Figure ??, you can see the qualitative behaviour of the Polder susceptibility $\chi(\omega)$ around the resonance frequency ω_{res} .

6.2 Kittel Formula

Most macroscopic ferromagnets have two opposite favorable directions in which they are most easily magnetized. The so-called easy-axis, which is parallel to the two directions, can be of different origin. In the following simplest case the sample shape anisotropy is treated. Here the magnetic field \vec{H} can be written as follows:

$$\vec{H} = \vec{H}_0 + \vec{H}_{\text{demag}} + \vec{h}(t). \quad (6.8)$$

The demagnetization field is given by $\vec{H}_{\text{demag}} = \vec{N} \cdot \vec{M}$, where the spatially independent demagnetization tensor \vec{N} is in diagonal form, with elements $N_{x,y,z}$. The resonance frequency can be written as

$$\omega_{\text{res}} = \gamma\mu_0 \sqrt{(H_0 + (N_y - N_z)M_0)(H_0 + (N_x - N_z)M_0)}, \quad (6.9)$$

if the applied magnetic field is in the direction of the z -axis.

These demagnetisation factors $N_{x,y,z}$ are strongly dependent on the sample geometry. The three most common geometries are discussed below.

1. spherical geometry ($N_{x,y,z} = 1/3$).

$$\omega_{\text{res}}^\circ = \gamma\mu_0 H_0 \quad (6.10)$$

2. thin out-of-plane magnetized film ($N_{x,y} = 0, N_z = 1$).

$$\omega_{\text{res}}^\perp = \gamma\mu_0(H_0 - M_0) \quad (6.11)$$

3. thin in-plane magnetized film ($N_{x,z} = 0, N_y = 1$).

$$\omega_{\text{res}}^\parallel = \gamma\mu_0 \sqrt{H_0(H_0 + M_0)} \quad (6.12)$$

The ferromagnetic resonance frequencies are simulated in Figure ??.

If there are no other anisotropies than shape anisotropy, M_0 is replaced by the saturation magnetization M_s .

If uniaxial field anisotropy is present, H_0 is replaced by $H_{\text{eff}} = H_0 + H_{\text{ani}}$. For thin in-plane magnetized films, the uniaxial field anisotropy is typically on the order of a few mT.

At this point, it should be noted that we do not know with certainty whether the easy-axis in thin Co films is in-plane, because out-of-plane easy-axis is also possible. With a suitable substrate, such as Au or Pt, single-digit monolayers of Co, and a suitable cap, such as Au or Ag, out-of-plane magnetization of Co may be present. In addition, there are studies of Co films as thin as 40 nm that both at normal and oblique incidence of atomic current during electron beam evaporation Co always exhibit in-plane easy-axis. At this point, I suspect that Co exhibits robust in-plane magnetization and only shows out-of-plane magnetization under very special conditions.

Furthermore, it should be considered that superconductors, such as aluminum, have a critical magnetic field of only a few mT. Only for very thin films, in the single-digit nanometer range, aluminum can achieve an in-plane critical field in the Tesla range. To use a finite ferromagnetic resonant frequency, within the critical magnetic field, an in-plane geometry must be used.

6.3 Co-planar Waveguide

In order to generate an alternating magnetic field distribution \vec{h} I use a co-planar wave guide (CPW). The CPW consists of an inner conductor, with width w , an infinitesimal height and two neighboring ground pads. For further descriptions I use the laboratory reference frame, shown in Figure ??, with x perpendicular to the CPW plane, z in direction of the inner conductor and y being perpendicular to x and z .

Acknowledgement

Dankeschön und so.

Wer das lieSSt ist schlau. Haha!